



HAL
open science

**Crystal Structure, Hirshfeld Surface Analysis and IR
Analysis of
2-Amino-1,9-Dihydro-6H-Purin-6-One-Selenate-Water**

S. Baaziz, E. Poyraz, R. Benali-Cherif, W. Falek, B. Hannachi, N. Dege,
El-Eulmi Bendeif, N. Benali-Cherif

► **To cite this version:**

S. Baaziz, E. Poyraz, R. Benali-Cherif, W. Falek, B. Hannachi, et al.. Crystal Structure, Hirshfeld Surface Analysis and IR Analysis of 2-Amino-1,9-Dihydro-6H-Purin-6-One-Selenate-Water. *Journal of Structural Chemistry*, 2023, 64 (7), pp.1350-1359. 10.1134/S0022476623070181 . hal-04421741

HAL Id: hal-04421741

<https://hal.science/hal-04421741>

Submitted on 28 Jan 2024

HAL is a multi-disciplinary open access archive for the deposit and dissemination of scientific research documents, whether they are published or not. The documents may come from teaching and research institutions in France or abroad, or from public or private research centers.

L'archive ouverte pluridisciplinaire **HAL**, est destinée au dépôt et à la diffusion de documents scientifiques de niveau recherche, publiés ou non, émanant des établissements d'enseignement et de recherche français ou étrangers, des laboratoires publics ou privés.

Crystal Structure, Hirshfeld surface Analysis and IR Analysis of 2-amino-1,9-dihydro-6H-purin-6-one-selenate-water

Sonia Baaziz^{1,3}, Emine Berrin Poyraz², Rim Benali-Cherif³, Wahiba Falek³, Bouzid Hannachi³, Necmi Dege², El-Eulmi Bendeif⁴ and Nourredine Benali-Cherif^{5,6}

¹*Département des Sciences de la matière, Faculté des Sciences Exactes, des Sciences de la Nature et de la vie, Université Larbi Ben Mhidi, Oum El Bouaghi, 04.000, Algeria*

²*Department of Physics, Faculty of Sciences, Ondokuz Mayıs University, Samsun, 55200, Turkey*

³*Laboratoire des Structures, Propriétés et Interactions Interatomiques, Université Abbas Laghrour-Khenchela, 40000 Khenchela, Algeria.*

⁴*Université de Lorraine, CNRS, CRM2, 54000 Nancy, France*

⁵*Université de Jijel- Mohamed Seddik BENYAHIA, BP98 Ouled Aissa, 18000 Jijel, Algeria*

⁶*Académie Algérienne des Sciences et des Technologies (AAST). Villa Rais Hamidou Chemin Omar Kachkar El Madania, Algiers- Algeria*

Abstract

A new guanine complex was synthesized and the structure was elucidated by SXRD and IR spectroscopic methods. Single-crystal X-ray diffraction analysis (SXRD) was used to describe the crystal structure. Triclinic, in the space group P-1, with the following properties: $a=9.5945(3)$, $b=13.1171(3)$, $c=14.1905(3)$, $\alpha =79.756(2)$, $\beta =82.036(2)$, $\gamma =84.902(2)^\circ$, $V=1736.70(8) \text{ \AA}^3$, $Z=2$. N-H \cdots O, O-H \cdots O and C-H \cdots O hydrogen bonds connect the molecules in the crystal, creating a three-dimensional supramolecular framework. The title structure is stabilized by the intra and intermolecular strong hydrogen bonds, according to a Hirshfeld surface analysis of the recorded intermolecular interactions. For the title complex, the two main interactions are H \cdots O/ O \cdots H (36.5%) and H \cdots H (23.7 %).

Keywords: Selenic acid, Guanine complex; Synthesis, Crystal structure; IR analysis

Introduction

One of the four nucleotide bases of DNA, along with adenine (A), cytosine (C), and thymine (T):is guanine (G).Guanine bases on one stand pair with cytosine bases on the other stand within a double-stranded DNA molecule. Information in DNA is encoded by the four-nucleotide base's sequence. The symbol for it is a G or Gua. Guanosine is the name of guanine's nucleoside. It is a purine derivative made up of carbon and nitrogen atoms arranged in two rings. It can be found in a variety of places, including guano (collected bat, bird, and seal excrement), yeast, fish scales, and sugar beets. Protonated nucleobases have a significant role

in defining 3-dimensional crystal structures, mediating conformational variations, examining proper folding and stability, and facilitating catalysis. Because of their capital roles, nucleobases have generated considerable scientific interest since their discovery.

All these interesting properties led us to the synthesis of novel guanine proton transfer compounds. In this context, selenic acid has been chosen to combine with guanine.

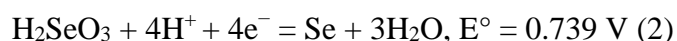
Recently, there has been a lot of research interest in designing and synthesizing organic-inorganic hybrid materials for their potential applications in catalysis, biochemistry, and crystallography [1].

Furthermore, organic–inorganic hybrid materials have been extensively investigated due to their considerable potential for scientific studies and technological applications, due to their capacity to combine important properties of organic materials (such as simple and easy synthesis method, structural variousness, easily adaptable structure and functional properties) and inorganic compounds (such as thermal, chemical and mechanical stabilities). Organic-inorganic hybrid materials can produce new functionalities from this combination. Moreover, these compounds exhibits a broad range of molecular interactions network, from strong ionic and hydrogen bonds to weak van der Waals contacts.

Among these hybrid systems, there are some notable arrays, including the formation of Guanine-selenic acid [2, 3, 4], and organic amines play an important role as structure directing agent in the hybrid organic-inorganic salts. In particular, the selenate and sulphate groups can form diversified structures with varieties of organic components and they are amenable for various functional applications [5, 6, 7].

Furthermore, selenic acid is an organic compound, with the chemical formula H_2SeO_4 , that can be found in over-the-counter daily dietary supplements as a source of selenium, an essential trace mineral for human health. It is a new inorganic electrolyte, which has great potential for practical applications owing to low porosity and high transparency of the resulting anodic oxide films [8, 9]. The first results on the aluminium anodizing in the selenic acid electrolyte were reported in 2013. It is easily soluble in water, dissolves metals such as silver, gold, and palladium [8]., and has a strong diacid property with dissociation constants similar to those of sulfuric acid $pK_{a1} = -3.0$, and $pK_{a2} = 1.7$.

Selenic acid solution dissolves silver, gold, and palladium metals [10]. Standard electrode potentials related to selenic acid are as follows:



Having all the motivations quoted above, we describe in this paper the first compound based on a protonated nucleobase with hydrogen selenate anion. According to the CSD data base (CSD Version 5.43, 2022) [10] no compound based on this anion with a protonated nucleobase has been reported so far, while only twelve compounds based on hydrogen selenate are known.

This study reports on the characterization of 2-amino-1,9-dihydro-6H-purin-6-one-selenate-water's structural parameters through single crystal XRD analysis, which were further confirmed by FT-IR analysis. We also analyzed the intra- and intermolecular hydrogen bonding interactions that stabilize the compound by discussing its graph-set descriptors. To complement these findings, we utilized a Hirshfeld surface analysis approach to examine intermolecular interactions. Through this technique, we were able to identify similarities and differences in the crystal structures of the compound using the associated 2D fingerprint plots.

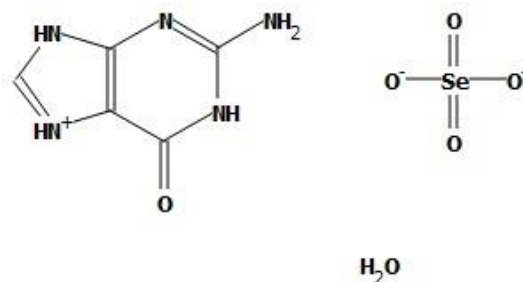
Experimental

Synthesis of The Title compound(ADPS):

All chemicals were bought and used as received. Selenic acid and Guanine are used in each experiment's synthesis process. Selenic acid was purchased from Sigma-Aldrich as solution (99.95%). Guanine was purchased from Alfa Aesar as solution (98%).

Single crystals of the compounds $(C_5H_6N_5O^+)(HSeO_4^-)$ were grown from aqueous solutions of Guanine and selenic acid, with 1:1:1 M.

Guanine (0.15g, 1.0 mmol) was dissolved in 10 ml of distilled water and reacted with an aqueous solution of H_2SeO_4 , H_2O (0.14g, 1.0 mmol). The mixture was stirred at 40° C temperature for 15 minutes. The reaction mixture was filtered, and the solution was allowed to slowly evaporate. The solution was crystallized in 10 minutes.



Scheme 1. Guanine and selenic acid.

SXRD Analysis

The asymmetric unit of the **ADPS** is shown in Fig. 1, and the complete crystallographic information is provided in Table 1. The asymmetric unit consists of 5 water molecules, 2 sulfate molecules and 4 2-amino-1,9-dihydro-6H-purin molecules. intramolecular hydrogen bonds are shown in Figure 1. The diffraction data of **ADPS** was collected with a Bruker APEX-II CCD diffractometer using monochromatic Mo-K α radiation ($\lambda = 0.71073 \text{ \AA}$) at $t 100(2) \text{ K}$. The structure was resolved using Olex2 [11] and Olex2. Using Charge Flipping and olex2, resolve [12] structure solution program. Using Gauss-Newton minimization, refine the [12] refinement package. In the structures, all of the hydrogen atoms were refined isotropically and placed in various Fourier maps. Anisotropic refinement was used for all non-H atoms. Table 1 contain information on **ADPS** 's crystal structure refinement as well as specifics on the bond lengths and bond angles. Mercury for Windows was used for creating the molecular and packing diagrams [13].

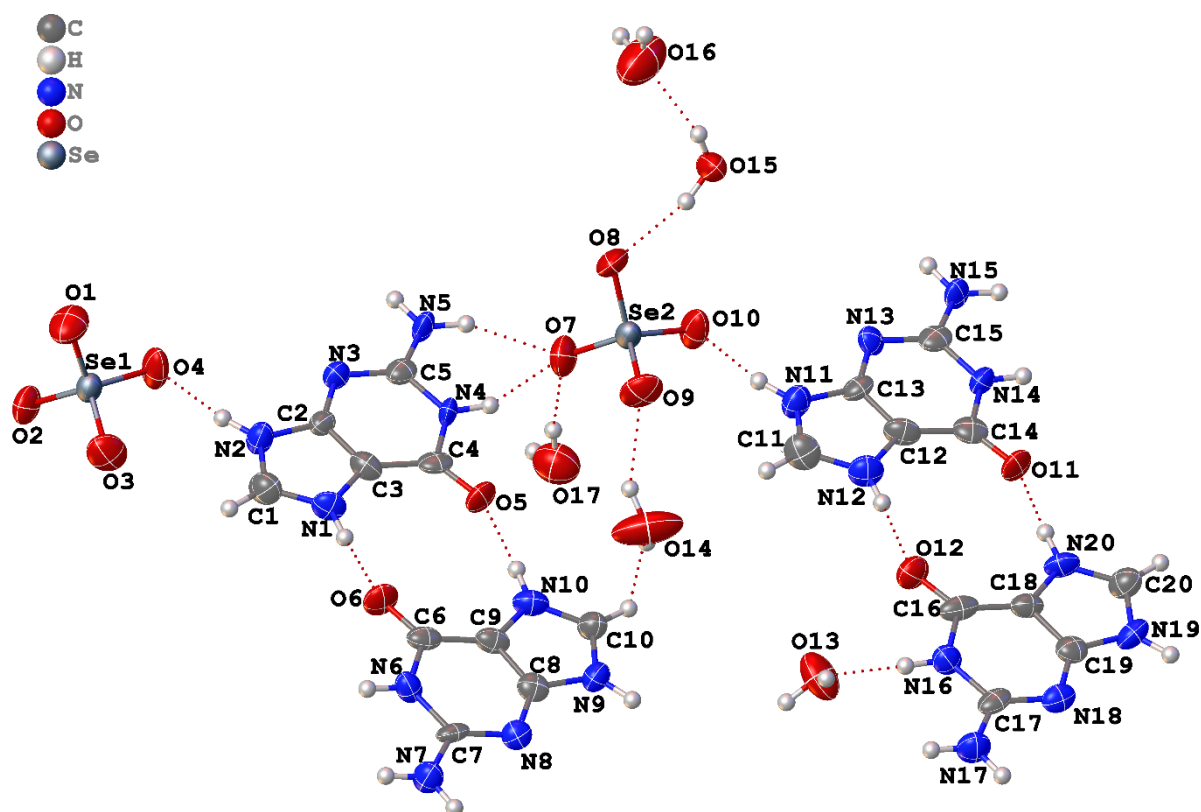


Fig.1. Ortep diagram of the molecule.

Hirshfeld Analysis

Crystal Explorer 17 was used to analyze the title compound's Hirshfeld surface [14,15]. The 3D surface mapped over d_{norm} for the range of 0.742 (red) to 1.530 (blue) a.u. is shown in Fig. 4a. If intermolecular interactions between atoms are made closer to the total of Van der Waals radii, a red spot is seen on the surface. When the surface is far from the sum of Van der Waals radii, it appears blue, and when it is close to the sum, it appears white.

IR Analysis

The FT-IR spectra of the title compound using KBr pellet were recorded in the range of 4000–400 cm^{-1} with a Bruker Vertex 80 V FT-IR spectrometer.

Results and Discussion

Crystal Structure of ADPS

Figure 1 depicts the molecular structure of $\text{C}_{20}\text{H}_{34}\text{N}_{20}\text{O}_{17}\text{Se}_2$ with atom numbers and as seen in Table 1, complex crystallized in a triclinic space group P-1 with a Z=2 composition. The structure of the complex shows that the organic guanine ligand performs proton transfer with selenic acid. Intramolecular and intermolecular O–H \cdots O and N–H \cdots O bonds stabilize the crystal packing of the complex in a three-dimensional network (Table 2). Selenic acid molecules extend like a chain with water molecules, and guanine molecules are located between these parallel chains (see Fig. 2).

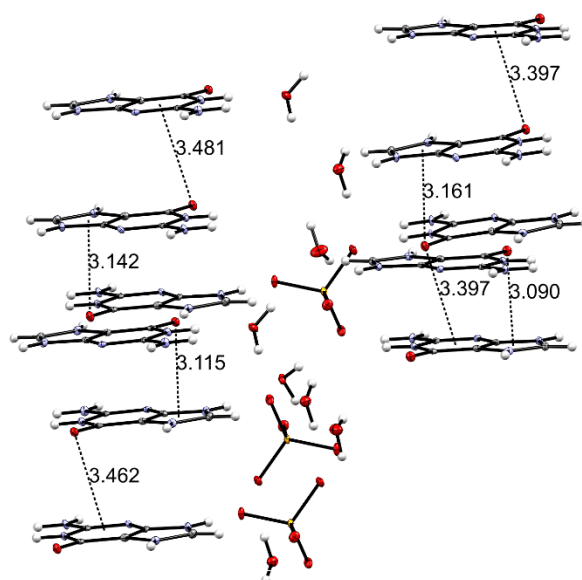


Fig.2. The dashed lines show the C=O... π interactions that form the crystal layers.

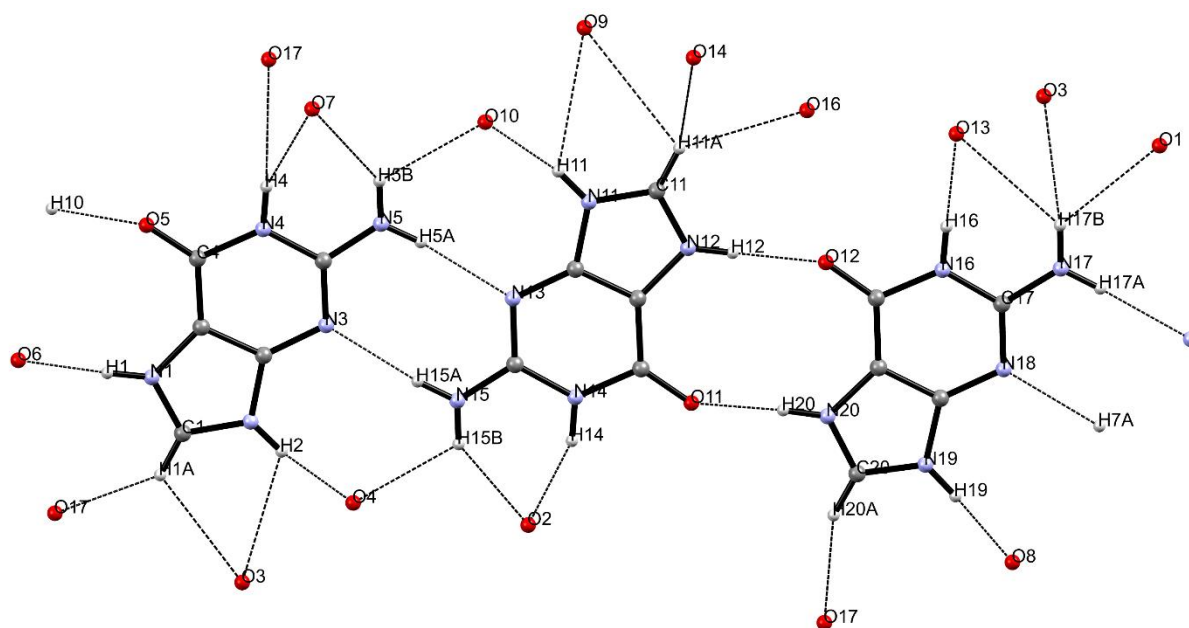


Fig.3. Hydrogen bonds.

Figure 3 clearly shows the hydrogen bonds for the crystal structure. $N2-H2 \cdots O4$ is the strongest bond. The bond lengths of selenium 1 and 2 with oxygens are given in the Table 3. Takouached et al stated in their work that the hydrogen diselenite anion ($HSe_2O_5^-$) is formed from two selenious acid groups (H_2SeO_3), that have a common oxygen atom as a bridge between two selenium atoms. This bridged selenium—oxygen distance is elongated with bond lengths of 1.8148 (14) Å and 1.8281 (14) Å for $Se1-O12$ and $Se2-O12$ respectively[16]. In this work, selenium—oxygen lengths were determined in the range of 1.634 to 1.651 Å.

Moreover, there are $C=O \cdots \pi$ interactions that form stacks of guanine molecules (Fig. 2, Table 4). Cg1 is the centroid of N1-C1-N2-C2-C3 ring; Cg2 is the centroid of N3-C2-C3-C4-N4-C5; Cg4 is the centre of N9-C8-C9-N10-C10 ring and Cg5, Cg7, Cg8, Cg10, Cg11 are the centers of N6-C6-C9-C8-N8-C7; N11-C11-N12-C12-C13; N13-C13-C12-C14-N14-C15; N19-C19-C18-N20-C20; N16-C16-C18-C19-N18-C17; respectively. Table 4 and Figure 2 clearly shows $C=O \cdots \pi$ interactions contribute to packing structure.

Hirshfeld Surfaces

Figure 4a shows the d_{norm} surface. The red spots appear because H bonds get the atom closer. As can be seen from here, the hydrogen bonds were effective in the structure. According to the existence of neighboring red and blue triangles, the shape-index, a tool for visualizing stacking interactions, is provided in Fig. 4b, while Fig. 4c displays the curvedness map of the title compound.

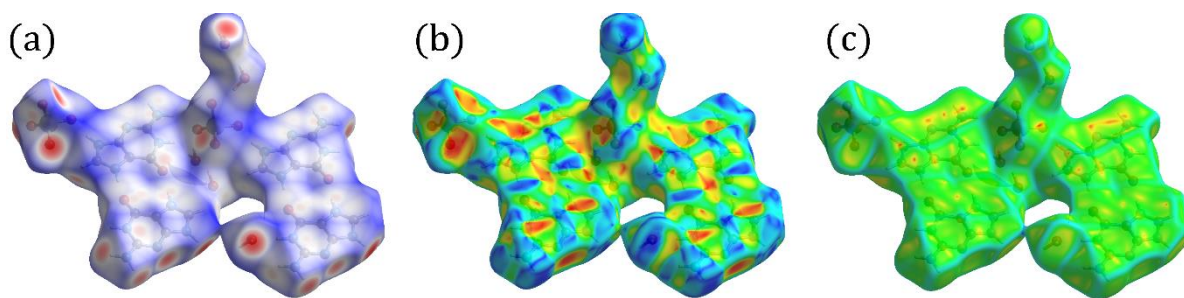


Fig.4. D_{norm} surface (a), shape-index (b) and curvedness surface of the title molecule (c).

The presence of prominent red and blue triangles in the shape index map confirms the presence of weak π - π interactions. Figure 5a show all interactions. The highest contribution to the Hirshfeld surface is from $\text{O}\cdots\text{H}/\text{H}\cdots\text{O}$ contacts with a 36.5 percent contribution

(Fig. 5b). Other interactions and their respective contributions are $\text{H}\cdots\text{H}$ (23.7%), $\text{N}\cdots\text{H}/\text{H}\cdots\text{N}$ (13.8%), $\text{C}\cdots\text{N}/\text{N}\cdots\text{C}$ (6.9%), $\text{C}\cdots\text{H}/\text{H}\cdots\text{C}$ (6.8%) and $\text{C}\cdots\text{O}/\text{O}\cdots\text{C}$ (6.1%). These are the most effective interactions and visualised in Fig.5 from b to g; respectively.

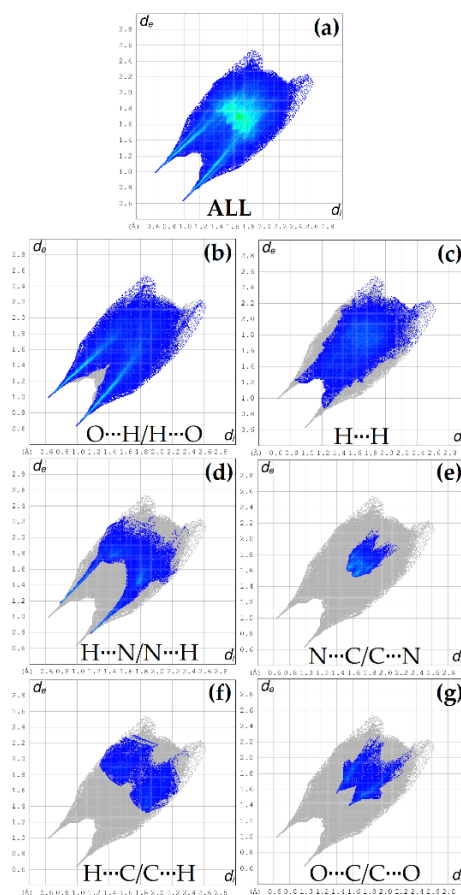


Fig.5. Fingerprint plots show atomic interactions.

Infrared (FT-IR) spectrum

Infrared (FT-IR) spectrum is a very powerful technique consists of characteristic bands of different functional groups, and it has been used to analysis structure and chemical bonding. In the IR spectrum of our compound, characteristic amide bands was observed. The first characteristic absorption band appeared at 3671 cm^{-1} was assigned to the N–H stretching vibration. Another band arising from the contribution of the scissor modes of the NH_2 groups was situated at 1648 cm^{-1} . The second characteristic strong vibrational band appeared at 2987.35 cm^{-1} was corresponding to =C-H elongation (benzene type). While the contribution of the stretching vibration of C = C groups was observed on the low-frequency side at 1609 cm^{-1} . Furthermore, the C=O stretching vibration was observed at $1650\text{--}1700\text{ cm}^{-1}$ in the infrared spectrum. In the $1300\text{--}1000\text{ cm}^{-1}$ region, the sample spectrum presents a series of bands with a maximum at 1066 cm^{-1} , indicate the presence of C-N stretching vibration.

Figure 6 shows the spectrum and peak lists.

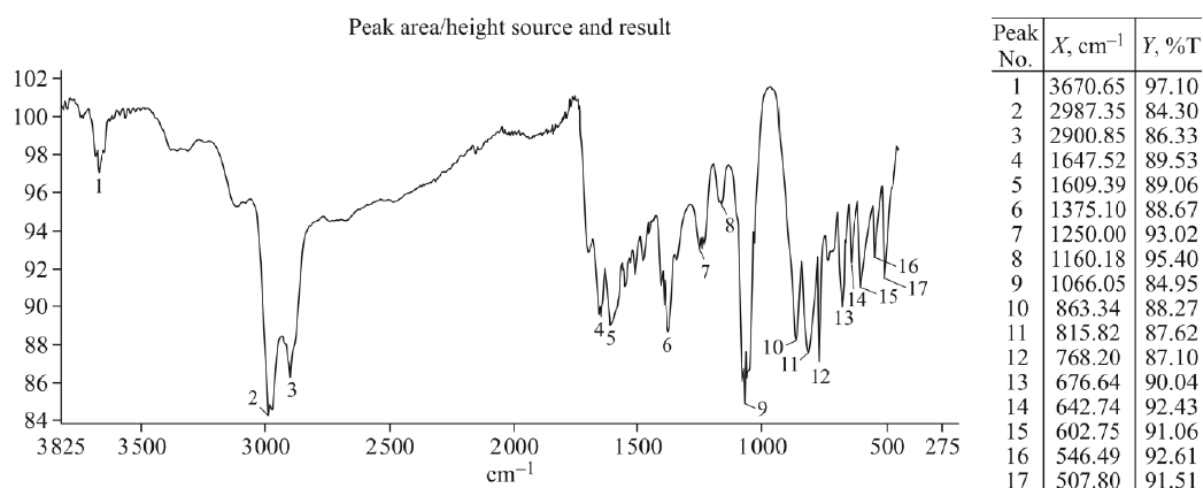


Fig.6. Fingerprint plots show atomic interactions.

Conclusion

A novel Guanine complex, 2-amino-1,9-dihydro-6H-purin-6-one-selenate-water, was investigated by single-crystal X-ray crystallography and IR spectroscopy. The X-ray findings show that the complex crystallized in a triclinic space group P-1 with a Z=2 composition. Intramolecular and intermolecular O–H···O and N–H···O bonds stabilize the crystal packing of the complex in a three-dimensional network. The results of the Hirshfeld surface analysis show that the major contribution to crystal packing comes from the O···H/H···O (36.5%) and H···H (23.7%) interactions.

Acknowledgments

The author acknowledges Ondokuz Mayıs University (Project number: PYO.FEN.1904.19.014) for the financial support of this research. We gratefully acknowledge the X-ray diffraction platform PMD2X of the Université de Lorraine for providing access to the X-ray diffraction facilities. We also thank the Algerian MESRS (Ministère de l'Enseignement Supérieur et de la Recherche Scientifique), DGRSDT (Direction Générale de la Recherche Scientifique et du Développement Technologique) and Abbes Laghrour Khenchela University, for financial support.

REFERENCES

- [1] Hagerman, P. J., Hagerman, D., Zubieta, J., *Organic–Inorganic Hybrid Materials: From “Simple” Coordination Polymers to Organodiamine-Templated Molybdenum Oxides*, 1999, 2, 181.
[https://doi.org/10.1002/\(SICI\)1521-3773\(19990917\)38:18%3C2638::AID-ANIE2638%3E3.0.CO;2-4](https://doi.org/10.1002/(SICI)1521-3773(19990917)38:18%3C2638::AID-ANIE2638%3E3.0.CO;2-4)
- [2] S.V. Krivovichev, V. Kahlenberg, R. Kaindl, E. Mersdorf, I.G. Tananaev, B.F. Myasoedov, *Nanoscale tubules in uranyl selenates*, *Angew. Chem. Int. Ed.*, 44 (7) (2005), pp. 1134–1136.
<https://doi.org/10.1002/ange.200462356>
- [3] S.V. Krivovichev, V. Kahlenberg, I. Tananaev, B. Myasoedov, *Uranyl selenates: from inite clusters to nanotubules*, *Acta Crystallographica A-Foundation and Advances*, 61 (2005).
- [4] S.V. Krivovichev, V. Kahlenberg, I.G. Tananaev, R. Kaindil, E. Mersdorf, B. F. Myasoedov *Highly porous uranyl selenate nanotubules*, *J. Am. Chem. Soc.* 2005, 127, 4, 1072–1073.
<https://doi.org/10.1021/ja0436289>
- [5] L. Nikhili, W. Rekik, H. Naili, T. Mihiri, T. Bataille *Crystal structures and characterization of two divalent metal selenates templated by dabco, (C₆H₁₄N₂) [M II (H₂O)₆](SeO₄)₂ (M II : Ni II, Zn II)*, *Arab. J. Chem.*, 10 (2017), pp. S2509- S2517, 10.1016/j.arabjc.2013.09.019.
<https://doi.org/10.1016/j.arabjc.2013.09.019>
- [6] O. Kammoun, T. Bataille, A. Lucas, V. Dorcet, I. Marlart, W. Rekik, H. Naili, T.M. Mhiri, *A supramolecular Double sulphate salt with lamellar type: crystal structure and thermal decomposition*, *Inorg. Chem.*, 53 (2014), pp. <https://doi.org/10.1021/ic402974k>
- [7] J.T. Rajamathi, N. Ravishankar, M. Rajamathi, *Delamination-restacking behavior of surfactant intercalated layered hydroxyl double salts, M₃Zn(OH)₈(surf)₂·2H₂O [M = Ni, Co and surf = dodecyl sulphate (DS), dodecyl benzene sulphonate (DBS)]*, *Solid State Sci.*, 7 (2005), pp. 195–99.
<https://doi.org/10.1016/j.solidstatesciences.2004.10.034>
- [8] O. Nishinaga, T. Kikuchi, S. Natsui, R.O. Suzuki, *Rapid fabrication of self-ordered porous alumina with 10-/sub-10-nm-scale nanostructures by selenic acid anodizing*, *Sci. Rep.* 3 (2013) 2748.
<https://link.springer.com/content/pdf/10.1038/srep02748.pdf>
- [9] T. Kikuchi, O. Nishinaga, S. Natsui, R.O. Suzuki, *Self-ordering behavior of anodic porous alumina via selenic acid anodizing*, *Electrochim. Acta* 137 (2014) 728.
<https://doi.org/10.1016/j.electacta.2014.06.078>
- [10] C.R. Groom, I.J. Bruno, M.P. Lightfoot, S.C. Ward, *Acta Cryst B* 72 (2016) 171–179.
<https://doi.org/10.1107/S2052520616003954>
- [11] O.V. Dolomanov, L.J. Bourhis, R.J. Gildea, J.A.K. Howard, H. Puschmann *J. Appl. Cryst.*, 42 (2009), pp. 339–341. <https://doi.org/10.1107/S0021889808042726>
- [12] L.J. Bourhis, O.V. Dolomanov, R.J. Gildea, J.A.K. Howard, H. Puschmann *Acta Cryst. A*, 71 (2015), pp. 59–75. <https://doi.org/10.1107/S2053273314022207>
- [13] C.F. Macrae, P.R. Edgington, P. McCabe, E. Pidcock, G.P. Shields, R. Taylor, M. Towler, J. van de Streek, *Mercury: visualization and analysis of crystal structures* *J. Appl. Crystallogr.*, 39 (2006), pp. 453–457. <https://doi.org/10.1107/S002188980600731X>

[14] Turner, M. J., MacKinnon, J. J., Wolff, S. K., Grimwood, D. J., Spackman, P. R., Jayatilaka, D. & Spackman, M. A. (2017). *Crystal Explorer 17.5*. University of Western Australia.

[15] Spackman, M. A. & Jayatilaka, D. (2009). *CrystEngComm*, 11, 19–32.

<https://doi.org/10.1039/B818330A>

[16] Takouachet, R., Benali-Cherif, R., Bendeif, E., Jelschb, C., Cherif, F. Y., Rahmouni, A. and Benali-Cherif, N. The supramolecular behavior and molecular recognition of adeninium cations on anionic hydrogen selenite/diselenite frameworks: A structural and theoretical analysis, *Journal of Molecular Structure*, 1229 (2021) 129836. <https://doi.org/10.1016/j.molstruc.2020.129836>

Table 1: Crystal data and structure refinement for ADPS

Empirical formula	C ₂₀ H ₃₄ N ₂₀ O ₁₇ Se ₂
Formula weight	984.536
Temperature/K	100.15
Crystal system	triclinic
Space group	P-1
a/Å	9.5945(3)
b/Å	13.1171(3)
c/Å	14.1905(3)
α/°	79.756(2)
β/°	82.036(2)
γ/°	84.902(2)
Volume/Å ³	1736.70(8)
Z	2
ρ _{calc} /cm ³	1.883
μ/mm ⁻¹	2.236
F(000)	996.5
Crystal size/mm ³	0.09 × 0.08 × 0.06
Radiation	Mo Kα (λ = 0.71073)
2Θ range for data collection/°	3.94 to 52
Index ranges	-14 ≤ h ≤ 14, -19 ≤ k ≤ 19, -20 ≤ l ≤ 21
Reflections collected	64370
Independent reflections	6826 [R _{int} = 0.1231, R _{sigma} = 0.0878]
Data/restraints/parameters	6826/1/541
Goodness-of-fit on F ²	1.081
Final R indexes [I ≥ 2σ (I)]	R ₁ = 0.0399, wR ₂ = 0.0995
Final R indexes [all data]	R ₁ = 0.0509, wR ₂ = 0.1066
Largest diff. peak/hole / e Å ⁻³	1.15/-0.87

Table 2: Hydrogen Bonds for The Title Compound

D	H	A	d(D-H)/Å	d(H-A)/Å	d(D-A)/Å	D-H-A/°
O15	H15c	⋯O8	0.8698	1.927(11)	2.766(3)	162(3)
O15	H15d	⋯O16	0.8700	1.965(9)	2.786(3)	156.9(19)
O13	H13a	⋯O1 ¹	0.8700	2.011(7)	2.869(3)	168(3)
O13	H13b	⋯O3 ²	0.8704	1.858(5)	2.723(3)	172(3)
O17	H17c	⋯O7	0.8700	1.905(3)	2.771(3)	173.8(16)
O14	H14a	⋯O9	0.8699	2.000(8)	2.788(3)	150.0(12)
N14	H14	⋯O2 ³	0.8800	1.913(3)	2.748(3)	157.79(9)
N4	H4	⋯O7	0.8800	1.904(3)	2.730(3)	155.66(10)
O16	H16b	⋯O2 ⁴	0.8699	2.023(7)	2.885(3)	171(4)
N19	H19	⋯O8 ¹	0.8800	1.748(3)	2.627(3)	176.17(11)
N1	H1	⋯O6	0.8800	1.781(3)	2.660(3)	177.17(10)
N12	H12	⋯O12	0.8800	1.833(3)	2.712(3)	176.48(10)
N9	H9	⋯O1 ¹	0.8800	1.852(3)	2.727(3)	172.17(10)
N6	H6	⋯O15 ⁵	0.8800	1.906(3)	2.755(3)	161.47(9)
N11	H11	⋯O10	0.8800	1.752(3)	2.621(3)	169.07(10)
N16	H16	⋯O13	0.8800	1.866(3)	2.744(3)	175.44(10)
N10	H10	⋯O5	0.8800	1.874(3)	2.751(3)	174.91(10)
N2	H2	⋯O4	0.8800	1.774(3)	2.647(3)	171.32(10)
N7	H7a	⋯O9 ²	0.8800	2.131(3)	2.893(3)	144.44(9)
N20	H20	⋯O11	0.8800	1.800(3)	2.679(3)	176.51(10)

Table 3: Bond lengths/Å

Atom	Atom	Length/Å	Atom	Atom	Length/Å
Se1	O3	1.634(2)	N9	C8	1.382(4)
Se1	O1	1.646(2)	N5	C5	1.331(4)
Se1	O2	1.637(2)	N17	C17	1.334(4)
Se1	O4	1.638(2)	N6	C6	1.391(4)
Se2	O9	1.629(2)	N6	C7	1.375(4)
Se2	O8	1.651(2)	N11	C11	1.337(4)
Se2	O7	1.644(2)	N11	C13	1.376(4)
Se2	O10	1.639(2)	N16	C16	1.395(4)
O12	C16	1.235(4)	N16	C17	1.372(4)
O6	C6	1.237(4)	N10	C10	1.318(4)
O5	C4	1.229(4)	N10	C9	1.385(4)
O11	C14	1.226(4)	N2	C1	1.338(4)
N14	C14	1.390(4)	N2	C2	1.373(4)
N14	C15	1.375(4)	N7	C7	1.333(4)
N3	C2	1.344(4)	N18	C19	1.350(4)
N3	C5	1.330(4)	N18	C17	1.331(4)
N4	C4	1.393(4)	N20	C20	1.321(4)
N4	C5	1.377(4)	N20	C18	1.382(4)
N19	C20	1.334(4)	N8	C8	1.350(4)
N19	C19	1.371(4)	N8	C7	1.328(4)
N1	C1	1.327(4)	C14	C12	1.419(4)
N1	C3	1.382(4)	C16	C18	1.411(4)
N13	C15	1.337(4)	C19	C18	1.376(4)
N13	C13	1.340(4)	C4	C3	1.420(4)
N12	C11	1.334(4)	C8	C9	1.365(4)
N12	C12	1.392(4)	C2	C3	1.377(4)
N15	C15	1.324(4)	C6	C9	1.415(4)
N9	C10	1.338(4)	C13	C12	1.380(4)

Table 4: C=O... π interactions

Atom-Atom -> ring centre	Symmetry	Distance / \AA
C4 -O5 -> Cg1	[i]	3.161(2)
C4-O5 -> Cg5	[ii]	3.397(2)
C6 -O6 -> Cg2	[iii]	3.474(2)
C6 -O6 -> Cg4	[iv]	3.090(2)
C14-O11 -> Cg7	[v]	3.142(2)
C14-O11 -> Cg11	[vi]	3.481(2)
C16-O12 -> Cg8	[vii]	3.462(2)
C16-O12 -> Cg10	[viii]	3.115(2)

[i] = -X,1-Y,1-Z ; [ii] = -X,1-Y,1-Z; [iii] = 1-X,1-Y,1-Z

[iv] = 1-X,1-Y,1-Z; [v] = 1-X,2-Y,-Z; [vi] = X,Y,Z

[vii] = -1+X,Y,Z; [viii] = -X,2-Y,-Z